

Mechanical properties of electroactive polymer microactuators with ion-implanted electrodes

Samuel Rosset; Muhamed Niklaus; Philippe Dubois; Massoud Dadras; Herbert R. Shea

Copyright 2007 Society of Photo-Optical Instrumentation Engineers.

This paper was published in Proceedings of SPIE Volume 6524 and is made available as an electronic reprint (preprint) with permission of SPIE. One print or electronic copy may be made for personal use only. Systematic or multiple reproduction, distribution to multiple locations via electronic or other means, duplication of any material in this paper for a fee or for commercial purposes, or modification of the content of the paper are prohibited.

Mechanical properties of electroactive polymer microactuators with ion implanted electrodes

Samuel Rosset^a, Muhamed Niklaus^a, Philippe Dubois^a,
Massoud Dadras^b, and Herbert R. Shea^a

^aEcole Polytechnique Fédérale de Lausanne (EPFL), Microsystems for Space
Technologies Laboratory, Lausanne, Switzerland;

^bInstitute of Microtechnology (IMT), University of Neuchâtel, Switzerland

ABSTRACT

We report on the use of the bulge test method to characterize the mechanical properties of miniaturized buckling-mode dielectric elastomer actuators (DEA). Our actuator consists of a Polydimethylsiloxane (PDMS) membrane bonded to a silicon chip with through holes. Compliant electrodes are fabricated on both sides of the membrane by metal ion implantation. The membrane buckles when a critical voltage is applied to the electrodes. The maximum displacements as well as the efficiency of such actuators strongly depend on the mechanical parameters of the combined electrode-elastomer-electrode layer, mainly effective Young's modulus E and residual stress σ . We report measured E and σ obtained from bulge tests on PDMS membranes for two PDMS brands and for several different curing methods, which allows tuning the residual stress by controlling the rate of solvent evaporation. Bulge test measurements were then used to study the change in membranes' mechanical properties due to titanium ion implantation, compared to the properties obtained from depositing an 8 nm thick gold electrode. At the doses required to create a conductive layer, we find that the Ti ion implantation has a low impact on the membrane's overall rigidity (doubling of the Young's modulus and reducing the tensile stress) compared to the Au film (400% increase in E). The ion implantation method is an excellent candidate for DEAs' electrodes, which need to be compliant in order to achieve large displacements.

Keywords: Dielectric elastomer actuator, bulge test, metal ion implantation, mechanical properties, PDMS

1. INTRODUCTION

Electroactive Polymers have generated wide interest because, despite their simplicity, they can develop large displacements (up to several hundreds percents) and reasonably high actuation pressure per unit mass (about $1 \text{ kPa} \cdot \text{m}^3/\text{kg}$).¹ EAP can be separated in two main sub-classes depending on their actuation mechanism: ionic EAP for which actuation is due to charge motion in an electrolyte, and electronic (or dielectric) EAP which are driven by an electrostatic force created between two electrodes separated by an elastic dielectric.² Dielectric EAPs (DEAPs) have the advantage of holding a given position without energy consumption, and only dissipate power when moving. In addition, since the electrostatic force scales as the inverse of the dielectric thickness, DEAPs are good candidates for miniaturization. Microactuators based on EAP enable a broad new range of applications for which large strains and forces are desirable, as their strain-force capabilities are not matched by any standard microactuators classes.

Dielectric EAP are basically an elastomeric polymer sheet sandwiched between two compliant electrodes.³ Applying a voltage between the electrodes creates a compressive electrostatic force which squeezes the film and, under free boundary conditions, causes the film's area to expand (Fig. 1). If the membrane's perimeter is fixed, no in-plane movement can take place, and hydrostatic compressive stress builds up in the membrane upon application of an electric field. Once the in-plane stress reaches the buckling limit, which depends on the membrane's geometry and mechanical properties, out-of plane deflection takes place with the formation of a bump whose height can be modulated by the applied voltage (Fig. 2).

In this paper we address the fabrication and mechanical characterisation of miniaturized buckling DEAP actuators (diaphragm actuators) based on a PDMS membrane bonded on a silicon chip with through holes.

Further author information: send correspondance to Samuel Rosset, samuel.rosset@epfl.ch, tel: ++41 32 7205437

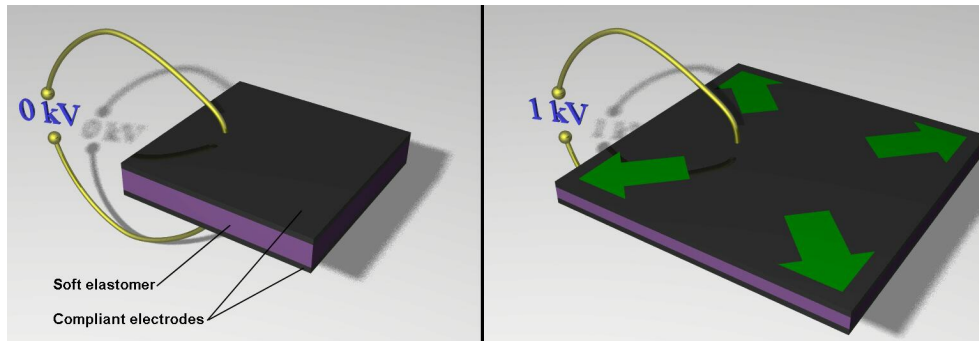


Figure 1. Dielectric EAP (DEAP) principle. When a voltage is applied to the electrodes (typically up to 1 kV), the electrostatic pressure squeezes the elastomer dielectric (right side). The volume of the dielectric being quasi constant, the whole structure stretches (in the case of free boundary conditions).

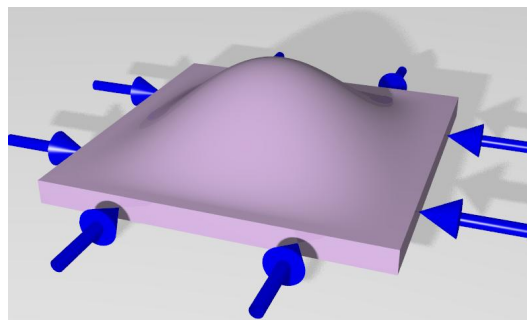


Figure 2. DEAP membrane with fixed boundary conditions (represented by the arrows) preventing the area expansion. Upon application of a voltage between the electrodes, hydrostatic compressive stress builds up in the membrane. When this stress reaches the buckling limit, out of plane deformation takes place and a bump is formed.

We show the advantage of metal ion implantation as a method to create patternable compliant electrodes. We show how bulge test can be used to measure the mechanical properties of thin PDMS membranes, and how the influence of the PDMS curing method and the technology used to produce the electrodes can be evaluated with this method.

One of the key factor to obtain large displacements with DEAs is to have compliant electrodes. Most of macrosized DEAs have electrodes made of conducting grease or powder (metal, graphite...)⁴⁻⁶ This method is not applicable to miniaturized DEAs for which the electrodes must be patterned on the micron-scale, in order to have many independently-addressable actuators. Standard *clean-room compatible* electrode creation methods, such as metal evaporation, tend to greatly increase the actuator's rigidity, which negatively affects its performance.⁷ However, we have showed on a proof-of-concept device that metal ion implantation allows the creation of very compliant electrodes that leads to vertical displacement of more than 10 % of the membrane's length.⁸

2. FILTERED CATHODIC VACUUM ARC IMPLANTATION OF METALLIC IONS

The field of low energy ion implantation into polymers remains little explored. A few publications report on resistivity reduction by ion implantation into rigid polymers.⁹⁻¹¹ Implantation into soft elastomers such as PDMS with the aim to create a conductive layer at the surface with a limited penetration into the sample (a few nm) requires an implantation at low energy (2 – 5 keV) to limit penetration of the ions and with a high flux to reach the targeted dose (about $10^{16} - 10^{17} \text{ cm}^{-2}$) in a reasonable amount of time. Conventional ion implanters cannot be used for that purpose, because it would take weeks to reach the desired dose at low energies. On the other

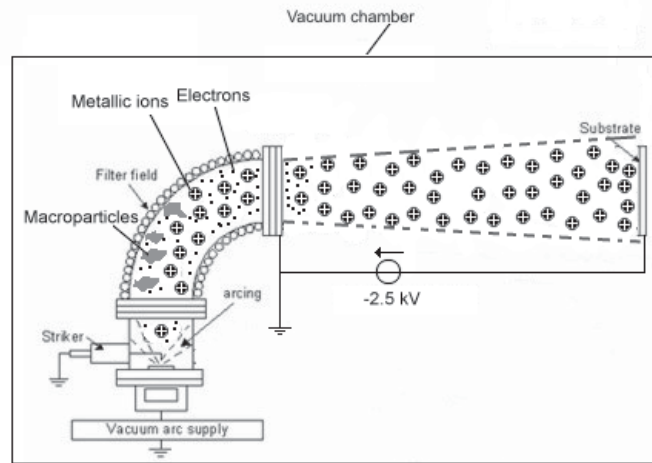


Figure 3. Schematic representation of FCVA implantation. Metal ions are created by pulsed cathodic arcs and are then magnetically deflected in a 90° bend to filter the ions from the large and heavy macroparticles which travel in a straight line due to their inertia and are lost at the duct walls. This ensures a high purity of the implanted species. The substrate holder is polarized at a negative potential of a few kV to accelerate the ions from the filter outlet to the target’s surface. (diagram adapted from www.nanofilm.com.sg)

hand, plasma based implantation can produce a high ion flux at low energies and is therefore a good candidate for DEAPs electrode fabrication.

Among the different plasma based methods, filtered cathodic vacuum arc (FCVA) (Fig. 3) is particularly interesting for DEAP electrodes: Its filtration system ensures implantation of pure ions with tunable energy and in contrast to plasma immersion ion implantation methods (PIII), pulsed FCVA does not submit the sample to constant plasma immersion. Consequently the temperature of the membrane remains low ($< 70^{\circ}C$). Indeed, due to the low heat conductivity of PDMS ($0.22 \text{ WK}^{-1}\text{m}^{-1}$ for Sylgard 186), thin PDMS membranes can easily burn if the implantation process generates too much heat. In the FCVA system we used (RHK Arc 20 system), $600 \mu\text{s}$ pulses were created at a frequency of 1 Hz. Implantation rate is relatively high and doses of 10^{16} cm^{-2} were obtained after 170 pulses (i.e. 170 s) for a surface resistivity of $3 \text{ M}\Omega/\square$.

3. MECHANICAL CHARACTERIZATION OF PDMS MEMBRANES

The performance of the buckling-mode actuators strongly depends on the mechanical and geometrical characteristics of the PDMS membrane. For example, the critical compressive stress, σ_{cr} , at which buckling occurs and the membrane starts to move is given, for circular plates under clamped boundary conditions, by¹²

$$\sigma_{cr} = 1.22 \frac{E}{1 - \nu^2} \left(\frac{t}{r} \right)^2, \quad (1)$$

where E the Young’s modulus, t the plate thickness, ν the Poisson coefficient (0.5 for elastomers, which deform without changing their volume), and r the membrane’s radius. This equation does not take into account the possible presence of residual stress in the PDMS layer. There is no analytical solution for rectangular plates, but a good approximation for square plates under clamped boundary conditions is given by¹²

$$\sigma_{cr} = 4.4 \frac{E}{1 - \nu^2} \left(\frac{t}{a} \right)^2, \quad (2)$$

where a is the side of the membrane. Below this compressive stress limit, the membrane does not move and is in a hydrostatic stress state. Consequently, below the buckling limit, the vertical compressive stress generated by

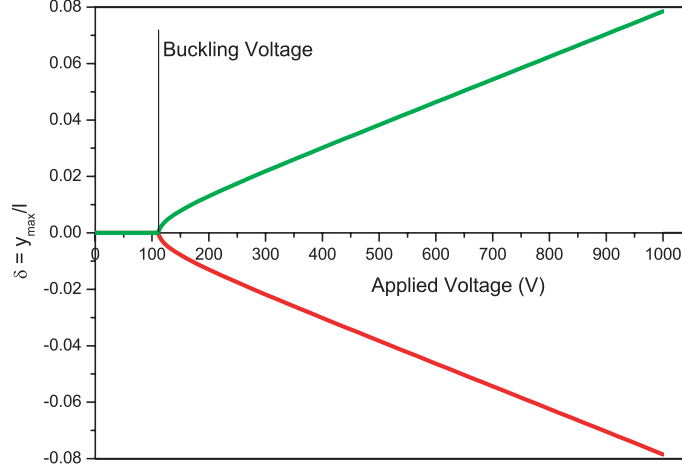


Figure 4. Numerical calculation of the normalized deflection of a clamped membrane's center point (deflection of the center over the membrane's side) based on energy minimization. A perfect membrane could either bend upwards or downwards, but in reality, the direction of the deflection will be imposed by initial defects of the membrane, such as initial bending. Calculations are made for a $3\text{ mm} \times 3\text{ mm} \times 25\text{ }\mu\text{m}$ square membrane with a Young's modulus of 1.5 MPa and a relative permittivity of 3.

the electrostatic field will be linked to the in-plane stress by the relation $\sigma_z = \sigma_{x,y}$. In EAPs, the vertical stress (electrostatic pressure) is given by³

$$\sigma_z = \epsilon_0 \epsilon_r \left(\frac{V}{t} \right)^2, \quad (3)$$

where ϵ_0 is the permittivity of vacuum, ϵ_r the relative permittivity of PDMS and V the applied voltage between the electrodes. Thus, the critical voltage (V_{cr}) needed to reach the elastic stability and obtain the formation of a bump can be calculated by combining Eqs. (1) or (2) with (3): $V_{cr} = \sqrt{(\sigma_{cr} t^2) / (\epsilon_0 \epsilon_r)}$. Postbuckling behavior can be numerically calculated based on energy minimization (Fig. 4) and also depend on the geometry of the membrane and its mechanical properties.

Geometrical characteristics of the membranes can be precisely determined: Their in plane size are defined by openings in a Silicon chip (Sect. 4) which are well controlled and thickness of the spun PDMS layer is measured on each chip using a Veeco optical profiler. The Young's moduli of the two tested PDMS were measured on macro-scale samples (cylinder $\phi 20\text{mm} \times 14.6\text{mm}$) by uni-axial compression tests on a well lubricated plate. Predicted actuator behavior using the above equations and Young's moduli extracted from compression tests and actual measurements on actuators showed some discrepancies. We obtained buckling voltages of 700 V⁸ when the theory predicted the limit of elastic stability at 200 V. Young's Modulus determination by compression tests has many limitations to predict the mechanical behavior of membranes, because it does not take into account the effect of solvent we have to add to the PDMS in order to spin-coat it (Sect. 4), and it gives no information on a possible residual stress, which can be present in the membranes. Consequently, an in-situ measurement of mechanical properties directly on the actuator's membrane is highly desirable to obtain valid data. We have built and used a bulge test setup in order to measure the Young's modulus and the residual stress of our membranes.

3.1. Bulge Test as a Means to Extract Mechanical Properties of PDMS Membranes

The bulge test is a technique developed for the determination of Young's modulus (E) and residual stress (σ_0) of thin films, such as SiN_x layers,¹³ metallic layers¹⁴ or rigid polymer layers.¹⁵ It consists in applying a gas pressure p on one side of a membrane placed on a sealed socket and measuring the vertical displacement Δz of its center. From the curve $p = f(\Delta z)$, and knowing the geometry of the membrane, it is possible to extract the values of E

and σ_0 . For circular membranes, the equation linking p to Δz is given by the following approximation:¹⁵

$$p = (1 - 0.24\nu) \left(\frac{8}{3}\right) \left(\frac{E}{1 - \nu}\right) \left(\frac{t}{r^4}\right) \Delta z^3 + 4 \left(\frac{\sigma_0 t}{r^2}\right) \Delta z. \quad (4)$$

For square membranes of side a , the approximation is given by:¹⁴

$$p = \frac{1}{0.792 + 0.085\nu} \frac{Et}{(1 - \nu)(a/2)^4} \Delta z^3 + 3.393 \frac{\sigma_0 t}{(a/2)^2} \Delta z. \quad (5)$$

These equations are valid for membranes whose surface is considerably bigger than their thickness. Finite element simulations (ANSYS) have shown that for a $30 \mu\text{m}$ -thick membrane, the above formulas are valid for our membrane of 3 mm (side or diameter) and 2 mm, but not for the smaller ones of 1 and 0.5 mm. Consequently, only the two biggest membranes have been used for the measurements reported here.

We have built a bulge test setup which is adapted to the measurement of soft PDMS membrane. Pressure is applied by a syringe pump through a 0.5 liter buffer volume in order to be able to apply pressure steps of the order of a few pascals. Pressure in the chamber is monitored by a barometric sensor (Intersema 5537) with a resolution of 1 Pa. Vertical displacement of the membrane's center is measured by a Veeco optical profiler (Wyko DMEMS NT1100). We took data points every 15 Pa from 0 to 600 Pa. The setup has been used to determine the mechanical properties of membranes made out of two different PDMS and under different environment during polymerization. In addition, as the bulge test is conducted directly on the PDMS membrane, it is also a very interesting tool to study the impact of the fabrication of the electrodes on the overall membrane's rigidity, by a bulge test measurement before and after the creation of the electrodes to quantify the increase of the Young's modulus and the internal stress modification due to the apport of conducting material on the membrane's surface.

4. SAMPLE FABRICATION

Circular and square holes were structured by DRIE in 4" silicon wafers. A patterned bilayer of $1.5 \mu\text{m}$ of SiO_2 and $8 \mu\text{m}$ of photoresist AZ1518 was used as an etching mask to drill holes through the $525 \mu\text{m}$ of the wafer thickness. The holes have a side length or diameter of 0.5, 1, 2 and 3 mm. The silicon wafers were then diced into $20 \times 20 \text{ mm}^2$ chips, each containing 4 square or circular holes of the above-mentioned dimensions.

PDMS layers are made by spin coating of commercially available PDMS diluted into isoocane to lower its viscosity. The two PDMS tested were Sylgard 186 from Dow Corning and Nusil CF19-2186. Due to the high viscosity of both PDMS (about $65 \text{ Pa} \cdot \text{s}$), a high solvent fraction needs to be used (typically 33-45 % wt.). The PDMS solution is spun on a polyvinylidene chloride (PVDC) film stretched on a rigid frame. This allows to spin-coat a PDMS layer on a deformable substrate, which is necessary to obtain a perfect bonding of the PDMS layer on the silicon chips. The PVDC substrate is treated in an oxygen plasma for 30 s to improve wetting characteristics. A $2 - \mu\text{m}$ thick photoresist layer (AZ1518) is spun on the PVDC film to serve as a sacrificial layer. After a 10' bake at 50°C to remove solvents from the photoresist, the PDMS is spin coated at 1200 rpm on the flexible substrate to obtain a layer PDMS layer about $20 - 25 \mu\text{m}$ thick (Fig. 5 a). Different curing methods have been used to polymerize the PDMS, such as Oven curing, curing under vacuum at room temperature and curing under a solvent-saturated atmosphere at room temperature. Curing methods have an influence on the evaporation of the isoocane from the PDMS solution, which impacts the final mechanical characteristics of the cured PDMS layer. The Si Chips are bonded on the PDMS membrane by RF oxygen plasma treatment:¹⁶ The Si chips and the membrane are put in a O_2 plasma reactor during 12s at low power ($\approx 250\text{W}$). They are then put into contact and left to bond during 2-3 hours. The assembly is then dipped into an acetone bath to dissolve the photoresist layer and release the chips from the PVDC substrate (Fig. 5 b).

Ti ion implantation has been conducted in an experimental setup which is only capable to implant a zone of a few cm^2 , thus explaining the need of a chip-level process rather than a wafer-level one. However, the steps describe above to obtain a thin membrane bonded on Si have also successfully been tested on entire 4" Si wafers. Topside implantation is carried out through a steel shadow mask (Fig. 5 c), but a photoresist mask patterned by photolithography could also be used on a wafer-scale process. Backside implantation is conducted without masks, through the silicon chip. Ti ions are deposited on the back of the membrane, but also on the edge of

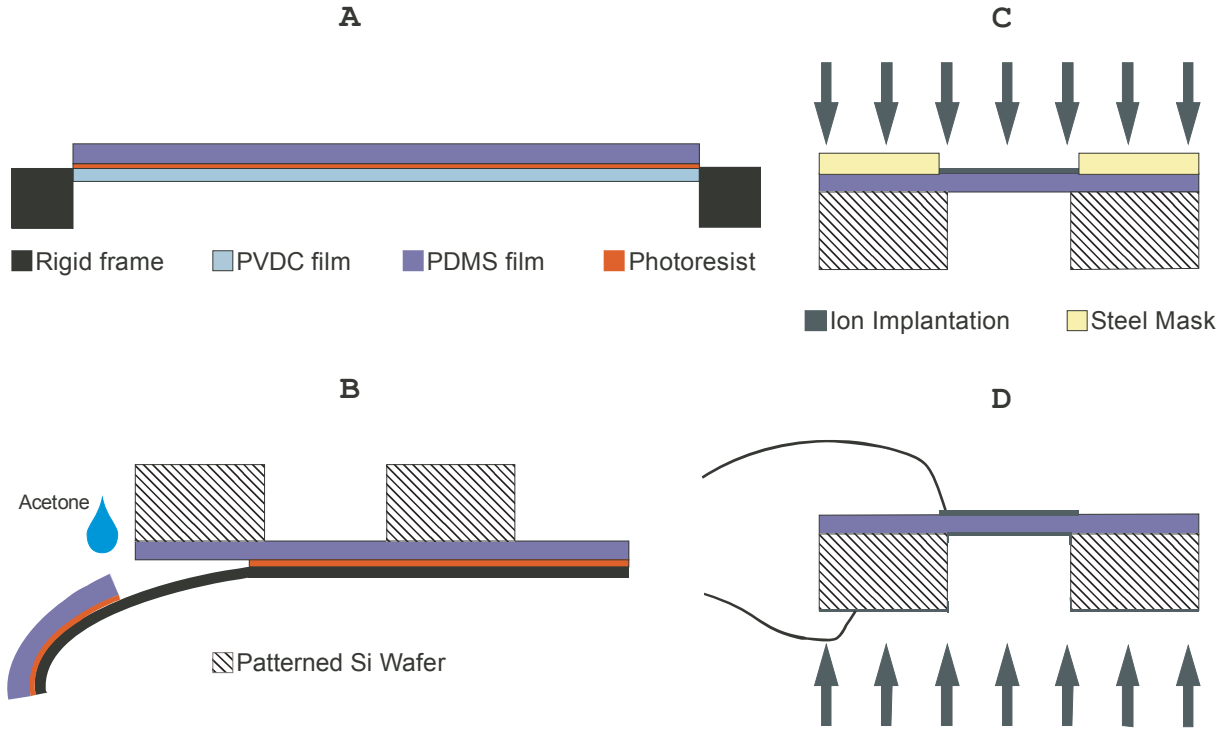


Figure 5. Process flow: A) Spin-coating on a deformable PVDC film of a 25 – 30 μm -thick PDMS layer on top of a sacrificial layer (photoresist). B) O_2 -plasma bonding of Si chips with through holes on top of the PDMS layer and separation from the PVDC substrate by dissolution of the sacrificial layer in acetone. C) Frontside Ti ion implantation using a steel shadow mask to define several independent actuators on each chip. D) Backside Ti ion implantation and electrical contacts.

the Si chip, thus ensuring electrical contact between the membrane and the chip, which can act as the ground during actuation (Fig. 5 d). Cathodic sputtering of gold layers between 8 and 15 nm has also been tested to compare the impact of this method versus implantation on the mechanical characteristics of the membranes.

5. MEASUREMENTS AND RESULTS

5.1. Influence of External Conditions During Polymerization

The first bulge test measurements we conducted on membranes that were polymerized in an oven at 100°C showed the presence of a large residual tensile stress (above 50 kPa). To control that phenomenon in our layers, we tested two other curing methods in addition of the oven: polymerization under vacuum in an attempt to remove the solvent from the PDMS before cross-linking occurs, and polymerization under a solvent-saturated atmosphere to keep the solvent in the PDMS during the polymerization and extract it afterward. Mechanical properties of membranes made with PDMS layers cured with the different methods described above were measured with the bulge test. Results are presented in Figure 6. Mechanical properties are found to be strongly dependent on the external conditions during polymerization of the PDMS. The Young's modulus is systematically lower than that of a macro-size sample, probably due to porosity induced by the presence and later evaporation of large quantities of isooctane. Polymerization under the solvent-saturated atmosphere produced layers that remained sticky and less resistant to deformation, and which also have an elasticity modulus much lower than that obtained with other curing methods; consequently it has not been pursued for now. For the remaining methods, membranes made out of Nusil CF19-2186 have a much smaller variation of its elasticity modulus, which remains very close to the value obtained for the macro-scale sample made without solvents.

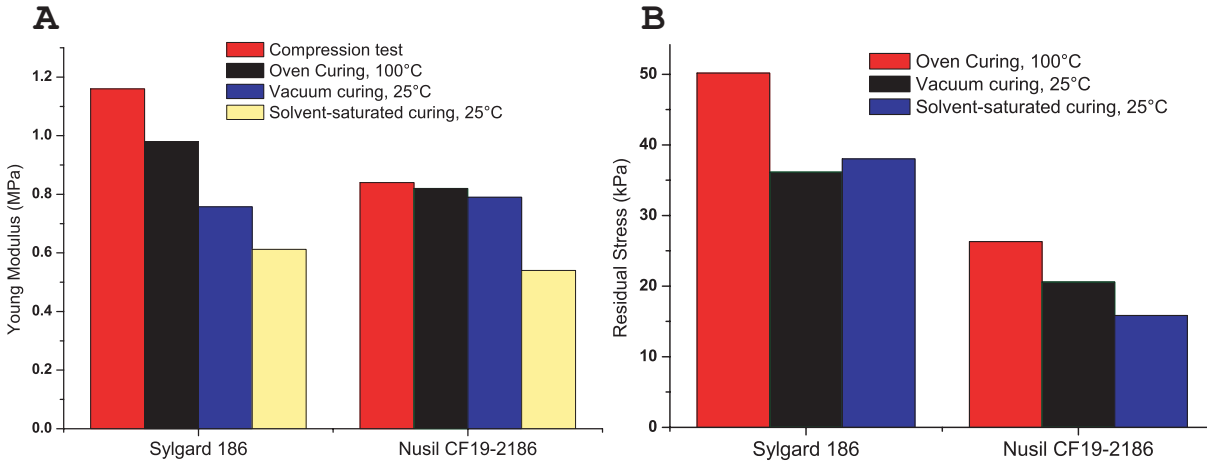


Figure 6. Comparison of properties for different curing methods and PDMS (Sylgard 186 and Nusil CF19-2186). A) Young modulus measured by uniaxial compression tests on a macroscale sample and with bulge test on membranes cured at 100°C in an oven, and at room temperature under a solvent-saturated atmosphere, or under vacuum. B) Tensile residual stress measured by bulge test on membranes under the same conditions as for A). Mechanical properties of the cured PDMS strongly depend on the environment during polymerization.

Residual stress results show that polymerization at high temperature in an oven induces large tensile residual tensions in the membrane, which is highly undesirable for it increases the buckling voltage limit. On some of the Sylgard samples with gold sputtered electrodes, we observed dielectrical breakdown before reaching the critical voltage at which the membranes starts to move. Nusil layers have lower residual stress than those made out of Sylgard. For vacuum-cured layers, the ratio of stress over Young's modulus is $2.6 \cdot 10^{-2}$ for Nusil and $4.7 \cdot 10^{-2}$ for Sylgard.

5.2. Influence of the Electrodes on Membranes' Properties

The Influence of conducting electrodes on the PDMS membranes was investigated by bulge test measurements. Pimpin et al. experimented on Sylgard 186 membranes with 200 nm evaporated Cr/Au/Cr structured electrodes with different coverage ratio in order to minimize impact on rigidity.⁷ Depending on the coverage area ratio, they obtained vertical displacement between 0.5% and 1.5% of the membrane diameter. In order to obtain larger displacements, we experimented with two different methods in an attempt to reduce the impact of the electrode on the membranes' rigidity: sputtering of ultra-thin layers of gold and FCVA Ti ion implantation.

A very-thin gold sputtered layer of 8 nm (percolation threshold) was deposited on a PDMS membrane and measured. Results show that even if the layer is very thin, an important increase in both Young's modulus (440%) and tensile residual stress (38%) occurs (Fig. 7 a), and gold adhesion on PDMS is very poor which makes the electrodes easily damageable. To make a working actuator, the backside electrode must also be deposited, which will further increase the membrane's Young's modulus and residual stress, thus explaining the very small displacements (a few percents) and the very high buckling voltage (above 1 kV, sometimes above breakdown voltage) we observed on actuators with gold-sputtered electrodes.

Titanium ion implantation was conducted on membranes in the FCVA apparatus for different amount of pulses (doses), ranging from 120 to 320 (Fig. 7 b). Chamber pressure during implantation was $2 \cdot 10^{-6}$ mbar and a negative bias of 2.5 kV was applied on the substrate holder. A complete calibration of the system remains to be done to correlate the number of pulses with the implanted dose. Preliminary RBS tests lead to a dose of $0.95 \cdot 10^{16}$ ions/cm² for 160 pulses and $1.05 \cdot 10^{16}$ ions/cm² for 180 pulses. Surface resistivity of Ti-implanted layers was measured on Sylgard PDMS layers which were spun on plain 4" Si wafers and implanted in a different FCVA system, capable of handling bigger substrates (Fig. 8 a). Even the smallest tested dose (10^{16} cm⁻²) produces layer sufficiently conductive to make functional actuators. An important dependence of the surface resistivity

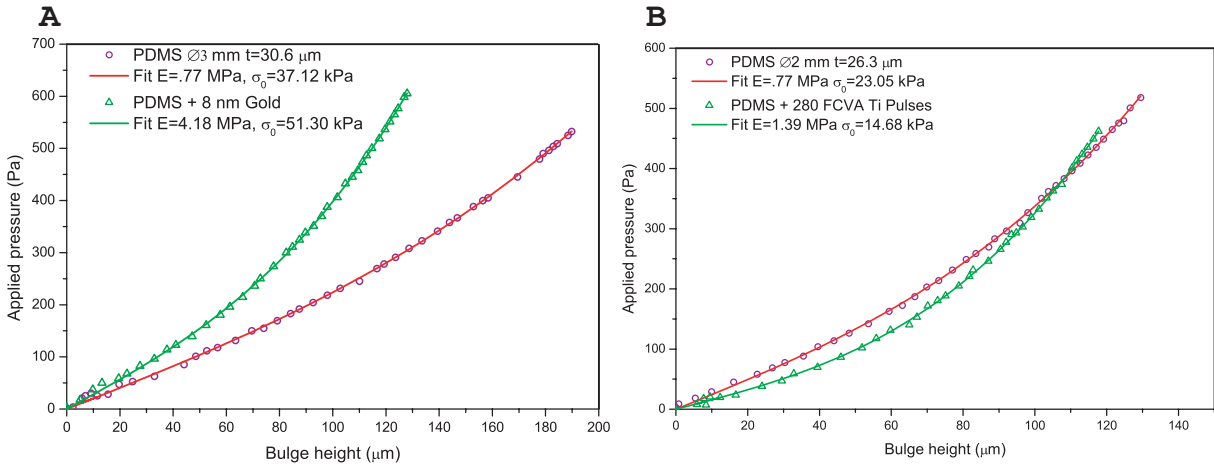


Figure 7. Comparison of the influence of metallic layer creation on a membrane's mechanical properties by bulge test measurement. A) Gold sputtering of a $8\mu\text{m}$ -thick layer. Deposition of the layer creates a relative increase of Young's Modulus over 440% and a relative tensile stress increase of 38% B) FCVA implantation of Ti ions with 280 pulses causes a lower impact on the Young's Modulus with a relative increase of 80%. Tensile stress is decreased by implantation (relative change of -36%) because of compressive stress building up at the membrane's surface due to metallic ions inclusion.

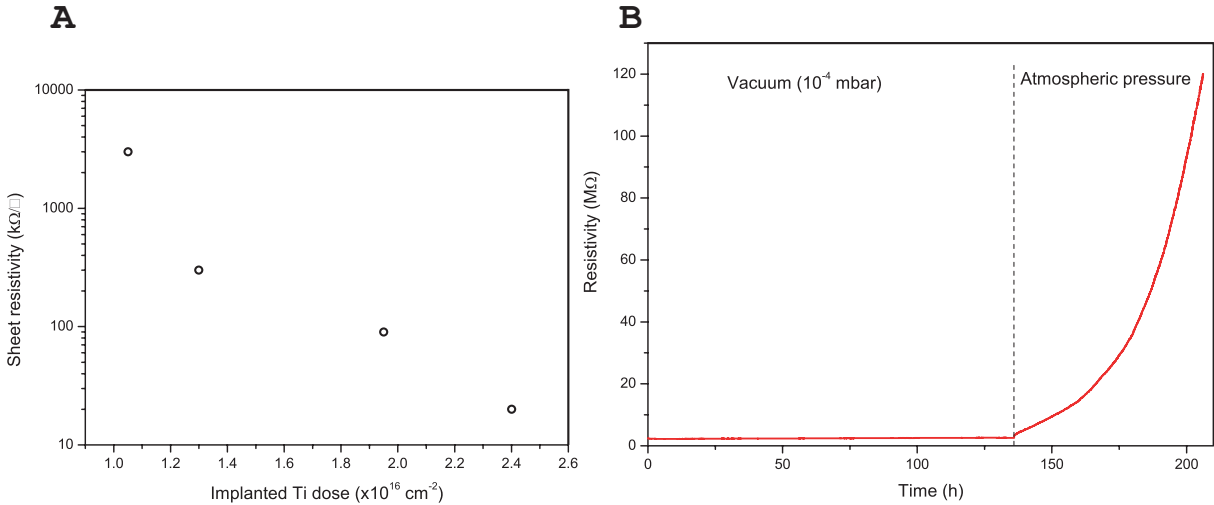


Figure 8. A) Sheet resistivity measurement on Ti-implanted PDMS layers for different ion doses. Resistivity obtained for the lowest dose ($3\text{ M}\Omega/\square$) is sufficient for proper actuation of the membranes. B) Degradation of implanted layer versus time. Sheet resistivity of a layer with 10^{16} cm^{-2} Ti was measured during several days. The layer was first kept under vacuum without noticeable degradation and later placed under atmospheric pressure with a dramatic increase in resistivity.

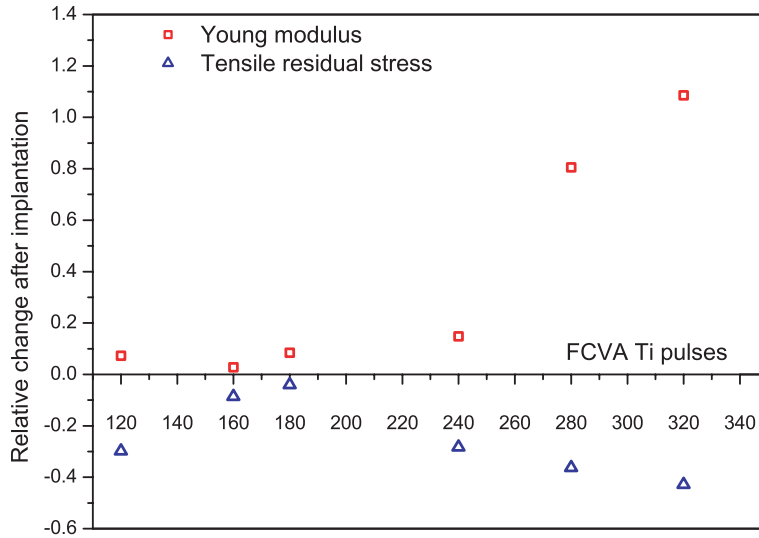


Figure 9. Relative change of Young's modulus and tensile residual stress for different number of arcs during Ti ion implantation. calibration remains to be done but preliminary RBS analysis show that a dose of 10^{16} ions/cm² corresponds to 160-180 pulses.

to time has been observed, as Ti is easily oxydized. Consequently, implanted layers are prone to degradation by diffusion of oxygen through the permeable PDMS (Fig. 8 b) and must therefore be kept under vacuum. Further testing of implantation with noble metals will be conducted to suppress this problem.

Results from bulge test measurements show that implantation has a much lower impact on the Young's modulus increase than sputtering, with a relative increase ranging from 10% to 110% for a single electrode (Fig. 9). Residual tensil stress is lowered from about 10% to 50% depending on ion dose, which is probably due to the creation of a compressive stress at the PDMS surface due to the inclusion of the metallic ions in the first few nm of the membrane. This is a welcomed side effect as it allows to lower the global tensile stress of the membrane created during polymerization, which in turn requires a lower actuation voltage.

5.3. Vertical Displacement under an Electric Field

Complete actuators with front- and basckside electrodes were manufactured and electrically actuated both statically and dynamically. Results for a square Sylgard 186 membrane of $3\text{ mm} \times 3\text{ mm} \times 26.3\text{ }\mu\text{m}$ polymerized under vacuum at ambient temperature and implanted with 320 pulses of Ti on both sides is given in Figure 10. Static measurements were conducted by applying a DC voltage between the two electrodes, and recording the vertical motion of the membrane's center with an optical profiler (Wyko NT 1100) (Fig 10 a). A moderate buckling voltage ($\approx 150\text{ V}$) is observed compared to what was observed on our first chips ($\approx 700\text{ V}$)⁸ whose PDMS membrane was polymerized at 100°C . The voltage was not increased until dielectric breakdown, so data do not show the maximal vertical displacement capabilities of this actuator. For dynamic measurements, a 0-200 V sinusoidal voltage was applied between the electrodes and the displacement of the membrane's center was recorded with a Polytec laser doppler vibrometer. The frequency of the AC signal was swept between 50 Hz and 5 kHz. Good response is observed from 50 Hz to 2.5 kHz, and the first mode mechanical resonance peak is clearly visible (Fig 10 b). Cut-off frequency of DEAP membranes is influenced both by the mechanical properties of the PDMS and by its electrical properties. High contact resistance between the electrical contact and the implanted electrode, or a not sufficiently-conducting electrodes can be factors that rise the electrical time constant.

6. CONCLUSIONS

We have shown that bulge test is an effective tool to measure the mechanical properties of thin PDMS membranes. Bulge test measurements have highlighted the fact that membranes made out of Sylgard 186 have a Young's

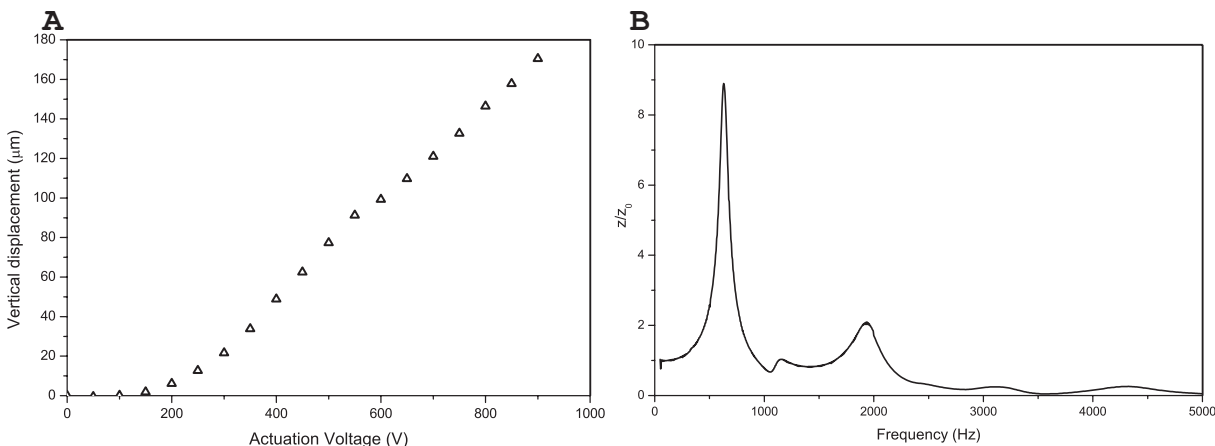


Figure 10. A) Static measurement of the vertical displacement of the center of a $3\text{ mm} \times 3\text{ mm} \times 26.3\text{ }\mu\text{m}$ Sylgard membrane with ion implanted electrodes (320 Ti pulses for top and bottom electrodes). Buckling voltage is approximately 150 V. Displacement was measured with an optical profiler. B) Dynamical measurement of the same membrane. A 0-200 V sinusoidal signal of varying frequency was applied between the electrodes and the ratio of the amplitude over the DC amplitude is reported for frequency between 50 and 5000 Hz.

modulus which is highly dependent on the curing temperature, and on the presence of the solvent. Membranes made of Nusil CF19-2186 show a smaller sensitivity to these factors. These measurements also showed the unexpected presence of residual tensile stress, which was dependent on the curing temperature. Tensile tensions in the membranes is undesirable, because it requires a higher voltage to make them move. Nusil CF19-2186 seems to be a promising PDMS for buckling mode (diaphragm based) DEA because of its reduced residual tensile stress relatively to its Young's Modulus.

We found that FCVA implantation of metallic ions had a reduced impact on the membranes' mechanical properties compared to very thin sputtered layers or to evaporated electrodes. Although implantation places the conductive particles below the PDMS surface, they are unfortunately subject to oxidation, because PDMS is permeable to gas. This causes Ti implanted layers to be subject to degradation, with a rapidly increasing surface resistivity if exposed to ambient air. FCVA implantation of noble metals could combine the advantage of ion implantation with insensitivity to oxidation.

ACKNOWLEDGMENTS

We thank Dr. Serguei Mikhaïlov and Mr. Johann Stauffer of the Ecole d'Ingénieurs ARC, Le Locle, Switzerland for the access to the FCVA implantation system.

REFERENCES

1. S. Ashley, "Artificial muscles," *Scientific American* **289**(4), pp. 52–59, 2003.
2. Y. Bar-Cohen, "Electro-active polymers: Current capabilities and challenges," in *Proceedings of SPIE - The International Society for Optical Engineering*, **4695**, pp. 1–7, 2002.
3. R. E. Pelrine, R. D. Kornbluh, and J. P. Joseph, "Electrostriction of polymer dielectrics with compliant electrodes as a means of actuation," *Sensors and Actuators A: Physical* **64**(1), pp. 77–85, 1998.
4. R. Heydt, R. Kornbluh, R. Pelrine, and V. Mason, "Design and performance of an electrostrictive-polymer-film acoustic actuator," *Journal of Sound and Vibration* **215**(2), pp. 297–311, 1998.
5. S. P. Lacour, H. Prahlad, R. Pelrine, and S. Wagner, "Mechatronic system of dielectric elastomer actuators addressed by thin film photoconductors on plastic," *Sensors and Actuators A: Physical* **111**(2-3), pp. 288–292, 2004.

6. F. Carpi and D. De Rossi, "Dielectric elastomer cylindrical actuators: electromechanical modelling and experimental evaluation," *Materials Science and Engineering: C* **24**(4), pp. 555–562, 2004.
7. A. Pimpin, Y. Suzuki, and N. Kasagi, "Micro electrostrictive actuator with metal compliant electrodes for flow control applications," in *Micro Electro Mechanical Systems, 2004. 17th IEEE International Conference on. (MEMS)*, pp. 478–481, 2004.
8. P. Dubois, S. Rosset, S. Koster, J. Stauffer, S. Mikhailov, M. Dadras, N.-F. d. Rooij, and H. Shea, "Microactuators based on ion implanted dielectric electroactive polymer (eap) membranes," *Sensors and Actuators A: Physical* **130-131**, pp. 147–154, 2006.
9. W. Yuguang, Z. Tonghe, L. Andong, Z. Xu, and Z. Gu, "Properties of implanted pet by w ion using mevva implantation," *Vacuum* **69**(4), pp. 461–466, 2003.
10. M. M. M. Bilek, P. Evans, D. R. Mckenzie, D. G. McCulloch, H. Zreiqat, and C. R. Howlett, "Metal ion implantation using a filtered cathodic vacuum arc," *Journal of Applied Physics* **87**(9), pp. 4198–4204, 2000.
11. J.-P. Salvetat, J.-M. Costantini, F. Brisard, and L. Zuppiroli, "Onset and growth of conduction in polyimide kapton induced by swift heavy-ion irradiation," *Physical Review B - Condensed Matter and Materials Physics* **55**(10), pp. 6238–6248, 1997.
12. W. C. Young, *Roark's Formulas for Stress and Strain*, McGraw-Hill, New York, 6th ed., 1989.
13. J. J. Vlassak and W. D. Nix, "A new bulge test technique for the determination of young's modulus and poisson's ratio of thin films," *Journal of Materials Research* **7**(12), pp. 3242–3249, 1992.
14. V. Paviot, J. Vlassak, and W. Nix, "Measuring the mechanical properties of thin metal films by means of bulge testing of micromachined windows," in *Materials Research Society Symposium - Proceedings*, **356**, pp. 579–584, 1995.
15. B. E. Alaca, J. C. Selby, M. T. A. Saif, and H. Sehitoglu, "Biaxial testing of nanoscale films on compliant substrates: Fatigue and fracture," *Review of Scientific Instruments* **73**(8), pp. 2963–2970, 2002.
16. J. J. McMahon, Y. Kwon, J. Q. Lu, T. S. Cale, and R. J. Gutmann, "Bonding characterization of oxidized pdms thin films," in *Materials Research Society Symposium - Proceedings*, **795**, pp. 99–104, 2003.